Shear induced structure in phase separated polymer solutions†

Carlo van Overbeek

August 28, 2013

Abstract

The behavior of phase separated polymer solutions under shear was studied by confocal microscopy in cone-plate and coaxial cylinder shear geometries. The observations were combined with macroscopic images, viscosity measurements and heterodyne light scattering velocity profiles. Wormlike banding, gradient banding and continuous phase inversion was observed for samples with a lower viscous dispersed phase at specific shear rates. Shear rates and strains were deduced to be heterogeneously distributed over banded samples as a function of the viscosity ratio between the separated phases. Shear strain and Laplace pressure seem to be the most important variables in determining the structure of a given system.

1 Introduction

Shear-thinning and shear-thickening of fluids or fluid-like systems are effects known to the scientific community for more than a century. Systems exhibiting these effects are usually referred to as non-Newtonian or complex fluids. Understanding the complex flow behavior of non-Newtonian fluids is of course an interesting research goal for fundamental science. But predicting and controlling the flow of such fluids is also of importance from an industrial point of view, as non-Newtonian behavior is also seen in most fluid products and intermiate products, such as ketchup, plastic and shampoo. The dawn of physical and colloidal science has enabled the community to synthesize, microscopically observe and perhaps understand these systems. In recent decades, the rheology of complex fluids has been studied on a molecular scale and effort has been made towards understanding their non-linear behavior under shear [1].

A peculiar subset within non-linear rheology is the shear banding effect [2], which can be considered as shear-enhanced phase separation of the system in multiple states differing in shear rate, shear stress, chemical composition, molecular ordering etc. The shear banding effect has been observed in a wide range of systems and efforts are being made towards connecting and understanding the underlying mechanisms [3, 4, 5]. (For newcomers, it would now be advisable to look at Figure 1, 2, 3 and 7 and/or leaf through the review articles cited above.) Most theories on banding flow are based upon coupling microstructural changes in a fluid with its rheological behavior. Also, gradient banding can usually simply be described by a separation of the system in a high and a low shear rate band. Yet, fully describing the banding behavior of fluids still poses a challenge to the field, both in experiment and theory.

Polymer solutions are a subset of the systems that can exhibit shear banding. Banding has been shown to occur in solutions of polystyrene in dioctyl phthalate [6] and phase separated solutions of polymers in water [7]. The banding of these systems might also be related to the reported string formation in polymer blends [8, 9]. In this research, the phase separated polymer solutions have been further investigated under shear. Less well-defined but still comparable systems can readily be found in the food industry (milk, mayonnaise, vinaigrette). These systems are subject to shear in their processing and consuming stage. This way, the observations made in this research may find application within processing of existing food products or designing new ones.

1.1 Definitions

Before describing the set-ups and experiments it is useful to introduce some terminology in general fluid mechanics. The simplest geometry to produce shear in shown in Figure 1. The direction of the shear is usually called shear gradient direction or sometimes simply gradient direction. Note that shear rate, velocity and vorticity all have a direction and are thus vector quantities. When a sample

† ***Master thesis***
Master programme:
Nanomaterials: chemistry & physiscs (Utrecht University)
Student:
Carlo van Overbeek BSc., 3235726
Supervisors:
dr. R. Hans Tromp (Nizo Food Research) &
prof. dr. Willem K. Kegel (Utrecht University)

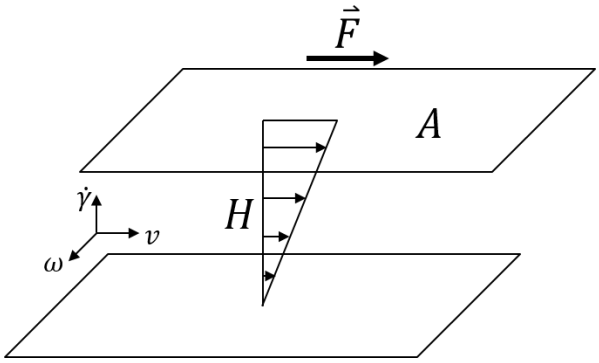

Figure 1: A schematic view of simple shear. The lower plate is held stationary, while the upper plate moves with a certain velocity. The sample between the plates is now sheared. The shear rate, $\dot{\gamma}$, is defined as the velocity difference between the plates divided by the plate separation distance, H. The shear stress, τ, is defined as the force used to move the upper plate divided by the surface area of the upper plate, A. Vorticity, ω, is defined perpendicular to both the direction of the shear rate and the direction of the fluid velocity, v.

shows inhomogeneities in only one of these directions that is called banding behavior. The direction perpendicular to the bands is the direction used to ascribe a type of banding behavior, Figure 2.

The shear stress, τ, set over a sample divided by the resulting shear rate, $\dot{\gamma}$, gives the sample's viscosity, η. Viscosity can be seen as a fluid's resistance to flow. A fluid is said to behave Newtonian when it has the same viscosity for any given shear rate or shear stress, i.e. a lineair relation between shear rate and shear stress. Also, Newtonian fluids do not prefer to let some regions in the fluid experience a higher shear rate than other regions. This last requirement for Newtonian flow is almost never met in shear banding fluids.

The dominant factor in determining the structure of phase separated polymer solutions under shear seems to be the ratio between the viscosities of the different phases present in a sample, the viscosity ratio. In this research, the viscosity ratio is defined as the viscosity of the continuous phase divided by the viscosity of the dispersed phase.

2 Experimental set-ups

Multiple set-ups have been used to investigate the behavior of phase separated polymer fsolutions under shear. The most often used set-up is cone-plate shear geometry combined with confocal microscopy, see Figure 3a for a schematic view of the set-up. In this type of set-up the cone and the plate are counter-rotating, so that the sample in the gap between the cone and the plate gets sheared. Because of the counter-rotation, somewhere between the two parts of the machine a plane exists which has zero velocity with respect to the outside world: the zero-velocity plane. By varying the ratio of rotation of the cone and the plate, the zero-velocity plane can be set to a desired height. A feature of rheology with cone-plate geometry is that the shear rate is the same at every point in the gap (if the sample behaves Newtonian).

The cone-plate set-up was custom assembled by Eltromat. The confocal microscope was manufactured by Leica. A list of the most important features of the set-up:

- Gap height at confocal microscope: 2 mm
- Depth up to which acceptable image quality is possible: 250 μm
- Cone angle: 4^o
- Lateral distance from cone tip to center of confocal microscope lens: 3 cm
- Cone cut-off: 50 μm

The other shear geometry used in this research is coaxial cylinder, present at Forschungszentrum Jülich. A schematic picture of which can be seen in Figure 3b. This shear cell is fully made of glass. The set-up uses normal fluorescence microscopy instead of confocal microscopy. Confocal microscopy is less advantageous in this set-up, because there is no zero-velocity plane. The shear rate is not completely homogeneous across the gap in this type of set-up. With the shear cells used, the shear rate at the outer cylinder is approximately 15 % lower than at the inner cylinder for all shear rates [12]. An advantage of this set-up compared to cone-plate

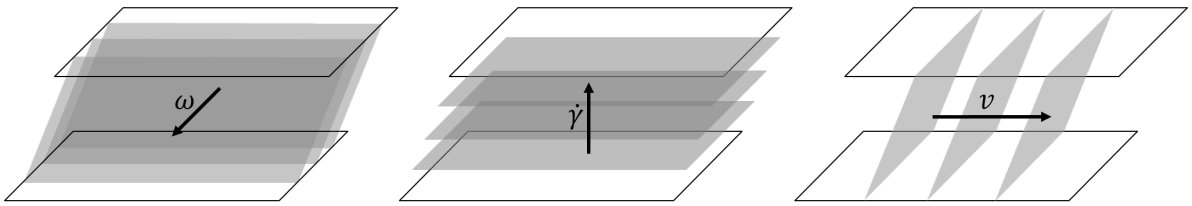

Figure 2: Schematic view of known forms of banding in a simple shear geometry. From left-to-right: vorticiy banding, gradient banding and flow banding. Flow banding will not be further considered beyond this point, as there is little literature available on the subject and it has not been observed in this research.

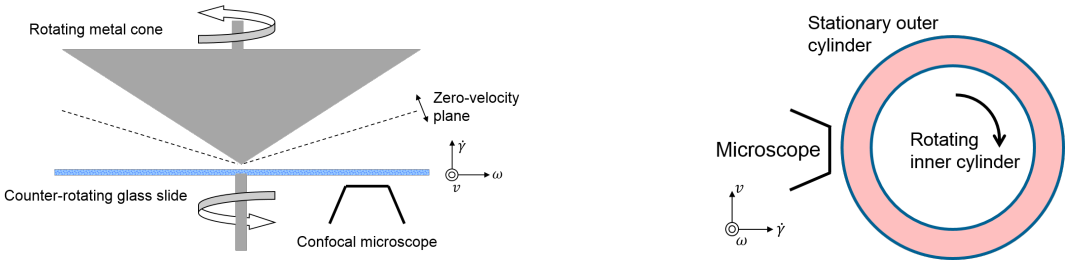

(a) **(b)**

Figure 3: Schematic images of **(a)** side side view of the cone-plate shear set-up and **(b)** top view of the coaxial cylinder set-up. Vorticity, gradient and flow direction are respectively denoted by ω, $\dot{\gamma}$ and v as in Figure 1. Note that these directions are defined from the point of view of the microscopes in the images.

is that the sample is macroscopically visible during the experiments. This makes simultaneously studying the sample at two orders of magnitude possible.

The set-up was custum assembled at Forschngszentrum Jülich. The microscope was manufactured by Leica, the detector by Photometrics, model: Coolsnap HQ. A list of some of the features of the coaxial cylinder set-up:

- Gap width: 1.5 mm
- Distance axis of rotation - outer cylinder: 24 mm
- Distance from inner cylinder - outer cylinder at the bottom (parallel plate geometry): ∼1 mm
- Inner cylinder filled with silicon oil for refractive index matching.

Besides fluorescence microscopy, this set-up can be rebuilt to do heterodyne light scattering experiments using a 1/1 beam splitter (Spectra Physics, Krypton laser $\lambda = 632$ nm). This changes the gap size from 1.5 to 2.0 mm. Heterodyne light scattering works by sending two laser beams through a sample and letting them interfere at various points along a line in the gradient direction. The light intensity that was not scattered while going through the sample is measured and variations in intensity between the two laser beams over time at a certain point in the sample are correlated. This way the velocity of the fluid at a certain point in a sample can be determined. The shear rate distribution within a sample can be determined by measuring multiple velocities, the difference in velocities over a distance equals the shear rate.

Viscosities were acquired by Ubbelohde measurements at 25 °C, using the Schott AVS 350 for automated measurement and the Schott CT 52 for temperature control. All samples were measured by Ubbelohdes with a capillary radius of 1.005 mm.

3 Gelatin/dextran solutions and emulsions

Gelatin and dextran polymers can both readily be dissolved in water. When solutions of gelatin and dextran are mixed, they can phase separate if the mass fractions of both polymers are high enough, Figure 4. The system then separates into regions with a high gelatin concentration and a high dextran concentration. In both phases, water is the most abundant component. Phase separation occurs at lower polymer fractions when increasing the length of the dextran polymer chains [10]. The phase separation depends little on temperature. Therefore the driving force behind the phase separation is believed to be based on entropy rather than enthalpy.

By shaking mixed solutions of gelatin and dextran the phase separated structure breaks up into a turbid suspension, which has the structure of an emulsion under microscopy, Figure 5. In these water/water emulsions either the gelatin rich phase or the dextran rich phase is the continuous phase. Predicting which phase will be continuous in these emulsions is not as straightforward as looking at the mass fractions of the added polymers, as will be seen later on. Of course, the true continuous phase in any of these solutions or emulsions is wa-

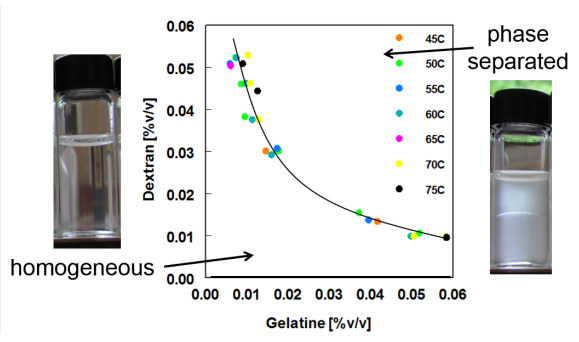

Figure 4: Phase diagram of gelatin/dextran solutions at multiple temperatures.

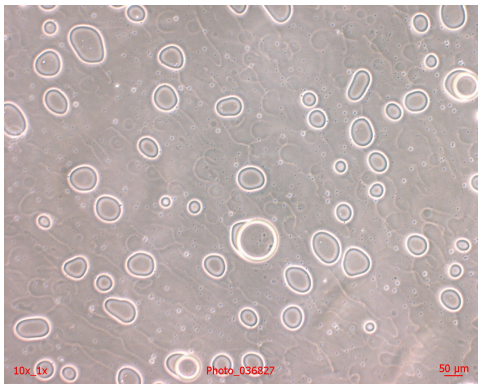

Figure 5: Normal microscopy image of a gelatin/dextran water/water emulsion between two glass slides. The dextran rich phase is continuous in this picture.

ter, but for all practical purposes from now on the abundant polymer in a region is used to ascribe a certain phase.

Just by looking at the microscopy picture of the emulsion in Figure 5, two things become clear. The first and easiest thing to note is that a gelatin rich droplet always seems to attach to the surface of air bubbles. Surface wetting appears to be a general feature of gelatin rich phases for a lot of surfaces; it also has been observed to wet water-metal and water-glass surfaces. Also the gelatin droplets in the picture are very non-circular in shape, especially compared to the air bubbles. This hints at a very low surface tension between the phases. This should be easy to understand by the fact that the most abundant molecule in both phases is still water and water has no surface tension with respect to itself. The surface tension between the two phases is in the range of 0.01 - 1 μN/m [7]. For comparison, the interfacial tension of water-triacylglycerol oil is 30 mN/m [11], which is a comparable system to vinaigrette without a stabilizing emulsifier.

Because both phases consist mostly of water and because gelatin and dextran differ not much from each other in density, both phases are about the same density. Sample tests have been performed to confirm this assumption and their density was indeed very close to that of each other. Both gelatin and dextran rich phases differ about 5 % in density from water at most. It should be noted though that the phases can change in (relative) density as a function of polymer fractions or sample salinities. This effect has not been addressed in this research. After macroscopic phase separation, the dextran rich phase is always the bottom phase in the samples used for this research, so these are slightly higher in density.

Liquid	**Viscosity (mPa·s)**
water	1
20 % dextran (37 kDa)	20
20 % dextran (150 kDa)	50
olive oil	100
20 % gelatin	250
20 % dextran (2000 kDa)	300
20 % pullulan	3000
honey	10000

Table 1: Viscosities of liquids used in this research and some reference liquids. Percentages are mass percentages of polymer dissolved in water. Viscosities of olive oil and honey were taken from [12].

As the gelatin and dextran phases have a low surface tension and differ little in density, they can form quite stable emulsions without a surfactant. Emulsions of short dextran chains usually take several hours to macroscopically phase separate. It can take several days before emulsions with long dextran chains phase separate.

In the introduction it has already been noted that the viscosity ratio is the most important variable in the research, see Table 1 for an overview of viscosities. Viscosities of polymer solutions vary greatly with polymer chain lengths. In this research the polymer chain length of the gelatin polymers will be kept constant and the chain length of the dextran polymers is varied. Samples in which the gelatin rich phase was the lower or higher viscous phase have both been tested to rule out effects specific to a either gelatin rich phases or dextra rich phases. Pullulan was used create dextran-like phases with a higher viscosity than gelatin phases. Pullulan is a linear polymer of glucose, whereas dextran is branched. The pullulan and gelatin used in this research are both about 200 kDa. Gelatin, dextran and pullulan solutions are weakly shear thinning, but not significantly in shear rate range at which the samples were studied (0.5 - 25 s^{-1}).

The gelatin used in this study is 'High Molar Weight Fish Gelatin' acquired from FIB Foods, all dextran polymers were acquired from SIGMA Life Science and the pullulan was acquired from Hayashibara. In microscopy experiments the gelatin rich phase was stained with Rhodamine B from Sigma-Aldrich.

4 Microscopic structure

The most obvious result of shearing emulsified gelatin/dextran solutions is that the shear stabilizes the emulsion structure. No macroscopic phase separation or sedimentation effects have been observed under low shearing conditions: $\sim$3 s^{-1}. A known effect is that shear stabilizes droplets which have an inner Laplace pressure which is on the same order of magnitude of the shear stress applied [14]. The Laplace pressure in droplets is defined by their size. Thus, to match the Laplace pressure to the shear stress, small droplets coalesce and large droplets break up. This standard behavior of emulsions un-

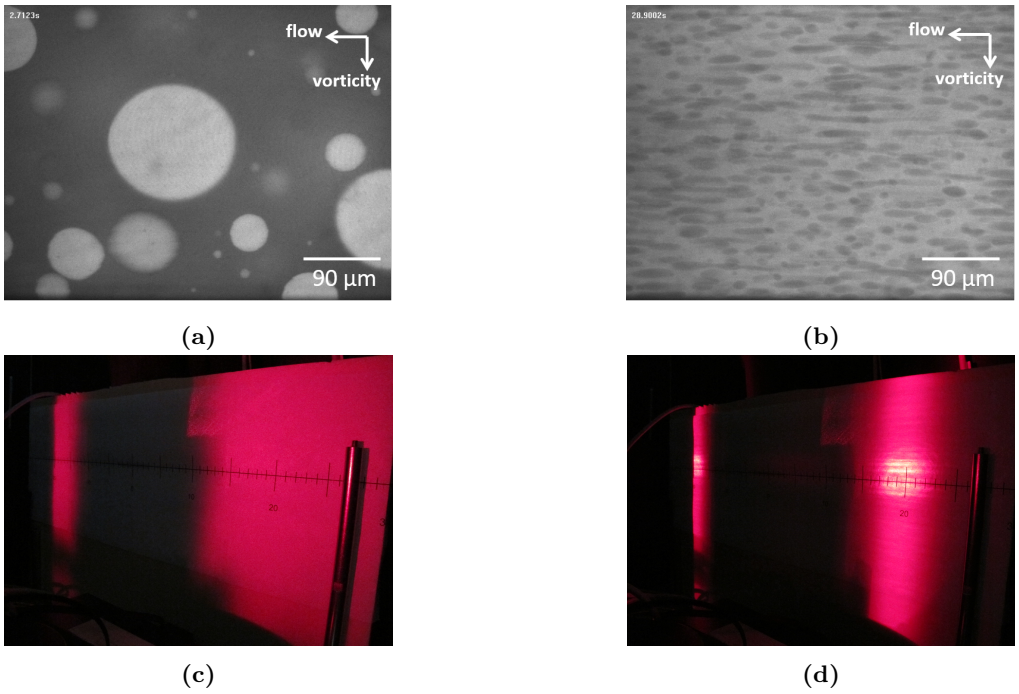

Figure 6: Observed effects of shear and viscosity ratio on deformation of droplets in an emulsion. **(a)** High viscosity droplets in a low viscosity continuous phase (gelatin : dextran 37 kDa = 1 : 3), shear rate $15\,s^{-1}$. **(b)** Low viscosity droplets in a high viscosity continuous phase (dextran 150 kDa : gelatin = 1 : 2), shear rate $10\,s^{-1}$. **(c)** Scattering profile of an emulsion with a lower viscous dispersed phase in a higher viscous continuous phase (gelatin : pullulan = 1 : 3) with no shear present. **(d)** Scattering profile of the same emulsion as in (c), but at a shear rate of $10\,s^{-1}$.

der shear holds quite well for gelatin/dextran emulsions under low shear conditions too.

When increasing the shear rate, the viscosity ratio between the continuous phase and the dispersed phase (droplets) plays a pivotal role in what happens next. The standard behavior of emulsions under shear still holds, when the viscosity of the continuous phase is lower than the viscosity of the dispersed phase, i.e. viscosity ratio smaller than unity. The droplets remain spherical in shape and their Laplace pressure is distributed around the shear stress at all shear rates tested ($0-25\,s^{-1}$), Figure 6a. Other effects start to happen to droplets with a lower viscosity than the continuous phase, i.e. viscosity ratio higher than unity, Figure 6b. At higher shear rates droplets start to exhibit a string-shaped morphology and a discrepancy between the shear stress and the Laplace pressure in the droplets starts to develop.

The only exceptions to these rules of thump are samples containing 2000 kDa dextran. Solutions of this polymer should be higher in viscosity than gelatin solutions of the same mass percentage (see table 1), yet not the gelatin droplets deform in a dextran continuous phase, but the other way around. It could be that dextran is a more swelling polymer than gelatin and takes up water from the gelatin phase. This would make the viscosity of the dextran phase actually lower than the gelatin phase. This hypothesis would need further research to be verified.

The deformation of low viscous droplets in a high viscous medium can also been concluded from light scattering experiments. In Figures 6c & 6d a laser bundle is shot through the same sample, but in Figure 6d shear is applied. The scattering profile is switchable within seconds from one to the other state by applying or stopping to apply shear. The scattering profile without shear is isotropic, typical for spherical microscopic structures. The scattering profile with shear is elongated in the vorticity direction of the sample, typical for microscopic structures that are elongated in the flow direction of the sample. These conslusions readily match the microscopy observations.

4.1 Banding

Wormlike banding

Emulsions of phase separated polymer solutions in which the dispersed phase deforms under shear can display banding behavior. Typically, the dispersed phase deforms when it has a lower viscosity than the continuous phase, i.e. viscosity ratio higher than unity (again save for the 2000 kDa dextran exception). Droplets of the dispersed phase first get elongated and even string-like under shear as

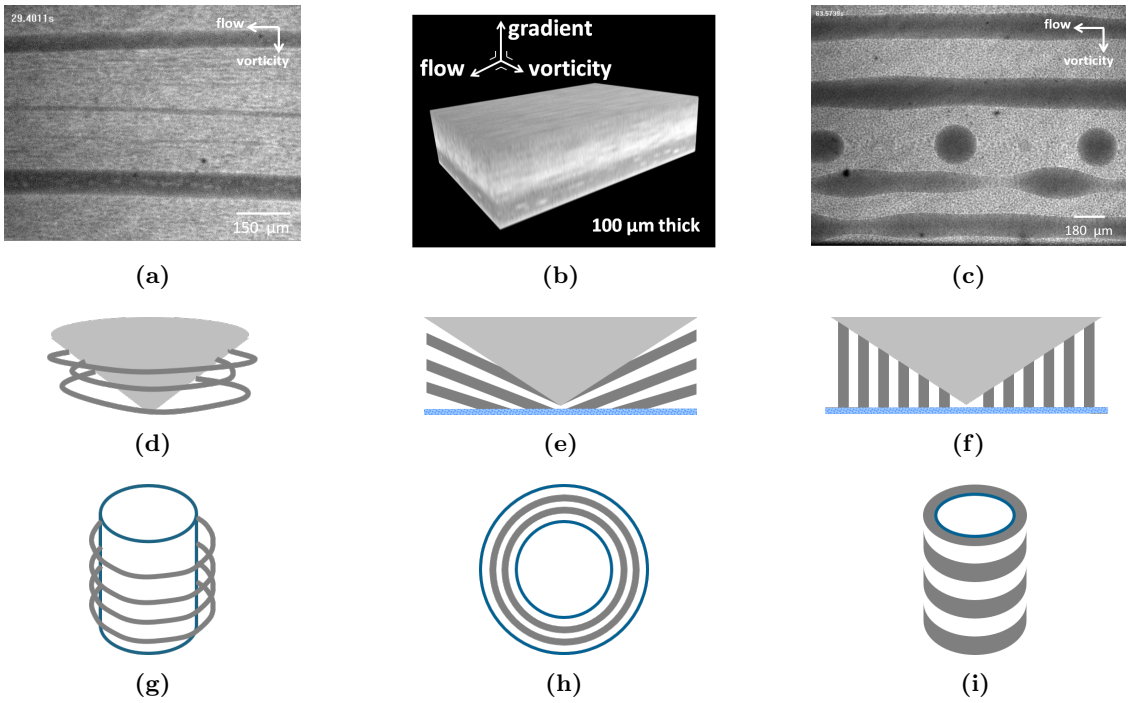

Figure 7: **(a)** In the middle of the picture string-shaped droplets are lining up to form a wormlike band, already formed bands are present on the top and bottom edges of the picture (dextran 2000 kDa : gelatin = 1 : 2, shear $5\,s^{-1}$). **(b)** Z-scan of a gradient band (dextran 150 kDa : gelatin = 1 : 3, shear $6\,s^{-1}$). **(c)** Bands breaking up 60 s after the shear is stopped (dextran 2000 kDa : gelatin = 1 : 3, shear was $15\,s^{-1}$). Note the Rayleigh-instabilities and satelite droplets. **(d/g)** Wormlike banding. **(e/h)** Pure gradient banding. **(f/i)** Pure vorticity banding. **(d-f)** Cone-plate set-up. **(g-i)** Coaxial cylinder set-up. **(d/g/i)** Isometric view. **(e/f)** Side cross section. **(h)** Top-down view.

seen in Figure 6b. Increasing the shear rate further causes the string-like droplets to line up on length scales much longer than their thickness. Eventually these droplets coalesce head-to-tail to form wormlike banded structures, Figure 7a. Observations using the coaxial shear set-up has shown that these bands span around the whole set-up like a torus. It is assumed that this also holds for the cone-plate set-up, because after many observations a band's 'head' or 'tail' have never been oberved. This would make wormlike bands look like schematically shown in Figure 7d & 7g.

Wormlike banded structures are stable under shear and become more stable at higher shear rates. They form at lower shear rates when more dispersed phase is present in a sample and/or when the viscosity ratio between the dispersed phase and the continuous phase is higher (i.e. the dispersed phase is much less viscous than the continuous phase). Wormlike bands have never been observed to coalesce or even bump into each other. Still, they clearly thicken with time. Whether this happens by coalescence with droplets or a process analogous to Ostwald ripening is still unclear. Another characteristic that has been observed is that wormlike banded structures form at much higher shear rates in a coaxial cylinder set-up than in a cone-plate set-up. This also holds for structures yet to be addressed (gradient banding, phase inversion). What causes this behavior is still unclear.

When lowering the shear rate, small wormlike bands immediately break up into droplets through Rayleigh-instabilities. This is a known effect for extended droplets [15]. Thicker bands have not been observed to break up at lowering the shear rate, possibly due to hysteresis in the formation of a banded state. When stopping the shear altogether, all bands break up, Figure 7c. With coaxial cylinder set-up it has been observed macroscopically that macroscopically visible bands break-up immediately at one spot when stopping the shear. Then they slowly break-up in droplets over their whole length almost simultaneously via Rayleigh-instabilities. Spinodal demixing has also been observed after quickly lowering the shear rate. This might be analogous to other sample types under shear reviewed in [9, 16].

When the shear rate is increased quickly after bands have broken up into droplets, the bands can form at much lower shear rates. Thus, the system has some sort of a memory for banding. This is probably due to the fact that the breaking up of wormlike bands results in relatively large droplets, as can be seen in Figure 7c. Due to a low surface tension between the coexsisting phases, these large droplets can sustain a highly deformed state for a

relatively long time upon restarting the shear. This would allow them to quickly reform wormlike bands. When the shear rate is increased slowly after an abrupt stop, the bigger droplets that were formed by bands breaking up get the chance to break-up into smaller droplets. This cancels out the memory effect and bands appear at their initial shear rates again. Upon reusing a previously sheared sample, the shear rate at which bands start to form appears to be slightly lower as well. Whether this is due to memory or another effect is not clear yet.

Gradient banding

In literature, bands are described that span the entire gap in the vorticity and flow direction, these are called gradient bands [4, 5], see Figure 2, 7e & 7h. Some gelatin/dextran 150 kDa samples have been observed to form gradient bands, Figure 7b. Just like wormlike bands, gradient bands form from a lower viscous dispersed phase. The shear rate of formation for gradient bands appears to be very close to, if not the same as, the shear rate at which wormlike bands start to form. The observed gradient bands are sensitive to changes in shear rate and shifts in the zero-velocity plane. When changes in either are applied too fast, gradient bands can break-up into large wormlike bands.

In the samples that perform gradient banding, it seems that one can endlessly cycle between a gradient banding state and a wormlike banded state. Gradient bands can be broken up in wormlike bands by fluctuating the shear rate. Gradient bands form when waiting long enough at a constant shear rate where wormlike bands are present. It seems that gradient bands form from wormlike bands slowly growing with time. As already mentioned, wormlike bands have not been observed to coalesce or bump into each other. This growing process without coalescence makes a process analogous to Ostwald ripening a likely way by which the gradient bands form from wormlike bands. Still, more time lapse and macroscopic research will have to be done to verify this hypothesis.

As mentioned in the text discussing Figure 5, gelatin rich phases tend to wet surfaces. By confocal microscopy it can be seen that under shearing conditions a gelatin rich phase is always bordering the glass slide, even when the dextran rich phase is the continuous phase in the rest of the sample. This wetting layer is typically a few tens of micrometers thick; more details about its thickness can be found in [20]. In dextran continuous samples the wetting layer can be seen as an ever present gradient band, but it is also a stable structure when there is no shear present, which is not the case for all other bands previously discussed. Because the wetting layer is not a structure that is formed or sustained by shear alone, it shall not be considered a true gradient band in the rest of this text.

Vorticity banding

Also described in literature are bands that span the entire gap in the shear gradient and flow direction, these are called vorticity bands [4, 5], Figure 2, 7f & 7i. Pure vorticity bands have not been observed in this research for any shear rate or waiting time and will therefore not be further considered beyond this point.

4.2 Inversion of phase continuity

Generally, the most abundant phase in an emulsion is also the continuous phase, but this can change when an emulsion is subjected to shear. When the viscosity of the sample is higher with the most abundant phase as continuous phase than with the dispersed phase as continuous phase, an inversion of phase continuity can occur [17, 18]. Inversions of continuity have also been observed in this research. Emulsions of phase separated polymer solutions can display this behavior when the dispersed phase has a lower viscosity than the continuous phase, i.e. a viscosity ratio larger than one. Inversion has not yet been observed in the coaxial cylinder set-up. This is probably ralated to the fact that banding also happens at higher shear rates there. It seems plausible that with other samples or higher shear rates this behavior can be triggered as well, but this is still to be verified.

Of course, samples with smaller viscosity ratios between the continuous and dispersed phase or smaller volume fractions of dispersed phase require higher shear rates to perform inversion of the continuous phase. Inverted emulsions can invert back to having the most abundant phase continuous again when the shear is stopped or lowered. This back-inverting happens at significantly lower

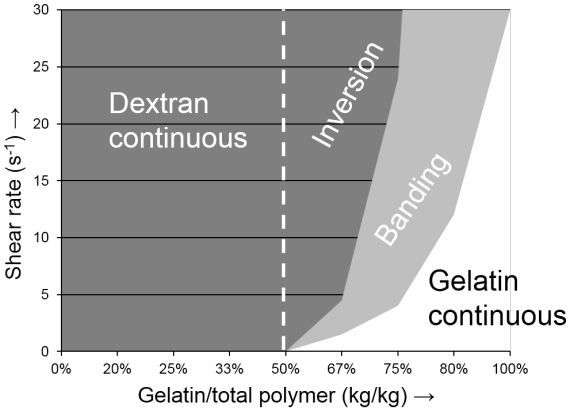

Figure 8: State diagram of 20 % polymer emulsions of gelatin/dextran 150 kDa under shear in cone-plate geometry, viscosity ratio gelatin : dextran 150 kDa = 5 : 1.

shear rates than the rate at which the inversion initially happened, so the process involves some kind of hysteresis and consequently has an activation energy.

By combining the data for continuous phase inversion and band formation a state diagram of the system under shear can be made, Figure 8. Although this diagram is specific for gelatin/dextran 150 kDa emulsions in cone-plate geometry, preliminary experiments suggest a similar lay-out for other emulsions containing gelatin and dextran with other molar weights or pullulan.

4.3 A link to overall viscosity

Viscosity measurements of the phase separated polymer solutions were performed by Ubbelohde. A theoretical average shear rate during the measurement can be calculated. These shear rates are much higher than the ones that could be produced in the shear sep-ups [19]. Still, the data produced by both techniques can be correlated well enough to allow further discussion.

Figure 9 shows the viscosities of gelatin/dextran 150 kDa emulsions as a function of the polymer mass ratio's in a sample. (The viscosities are of the same type of samples as those used to acquire the data for Figure 8.) When looking at Figure 8 it can be seen that phase inversion is possible to about 75 % gelatin. In Figure 9a it can be seen that the steepest increase in viscosity with increasing gelatin percentage is also at about 75 % gelatin. From this correlation it can be deduced that the viscosities in this set of samples are linked to the microscopic structures. Under shear the system prefers to have the lower viscous phase as the continuous phase, even when the lower viscous phase is not the majority phase. It can also be deduced that the continuous phase has a bigger influence on the overall viscosity of the sample than the dispersed phase. These results might be analogous to those observed in reference [13].

In Figure 9b the viscosities of the system in Figure 9a diluted to 15 % are shown. The most striking observation in this picture is that the overall viscosity goes down from an all dextran emulsion to one that contains 17 % gelatin polymer, whereas one would expect that adding a more viscous compound to any mixture should always increase the overall viscosity. Some hypotheses to explain this phenomenon have been formulated. It could be that the polymer chain statistics vary with the polymer concentrations. This might lead to stronger swelling of one type of polymers relative to other. This could lower the viscosity of the continuous phase by dilution and subsequently raise the viscosity of the dispersed phase. The overall viscosity would lower by this process, as the overall viscosity is determined more by the continuous phase than the dispersed phase. It could also be that the interfaces between the two phases are depleted from polymers, creating a layer of pure water in between them which has a very low viscosity. This depletion layer could let the two phases flow in concentric shear bands sliding along each other through the capillary. Still, for all given hypotheses more research would have to be done to verify any. Any awnser should also be able to explain why this process is not observed at 20 % polymer emulsions.

If the first and last data points (viscosities at 0 % and 100 % gelatin respectively) in Figure 9 are ignored, the viscosities of 15 % polymer emulsions show the same trend as the 20 % polymer emulsions: two linear regions separated by a ramp in viscosity. It seems likely that these 15 % polymer emulsions have an inversion of phase continuity beyond 75 % gelatin such as the 20 % polymer solution, but more experiments using the cone-plate set-up will have to be done to verify this hypothesis. This is why Figure 9b shows a dark grey area to signify the ramp in viscosity, but state desciptions as in Figure 9a are left out.

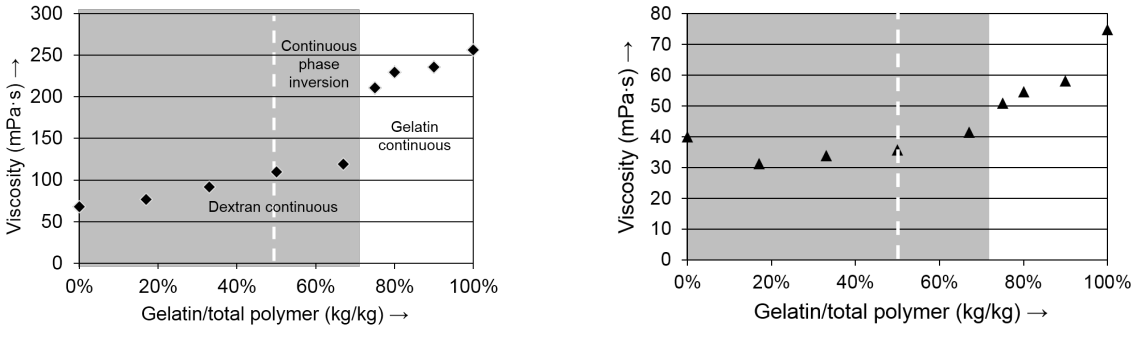

(a) **(b)**

Figure 9: Viscosities of gelatin/dextran 150 kDa emulsions, measured by Ubbelohde. **(a)** Viscosities of 20 % polymer emulsions. **(b)** Viscosities of 15 % polymer emulsions.

5 Macroscopic structure

With Figure 8, a first step has been set towards describing the different structures of gelatin/dextran emulsions under shear. However, the data for that figure was obtained only by microscopic techniques. So, the natural follow-up question is: do these structures correlate with macroscopic effects? In Figure 10, a macroscopic picture of a gelatin/dextran emulsion in the banded state can be seen. The picture shows a lot small of bands and correlates well with Figure 7a stacked in the vorticity direction. Also the bands extend around the whole set-up in the flow direction. This may be hard to see in the picture, because the bands are only visible at a certain angle of light incidence and point of view. But multiple other macroscopic observations indeed confirm that wormlike bands macroscopically look like thin donuts (i.e. a torus with $r_1 \gg r_2$).

Besides the small bands observed in Figure 10, other bands have been observed that stretch beyond the microscopic domain in the vorticity and flow directions, Figure 11a. A microscopic picture of the macroscopic border between two such bands is shown in Figure 11b. It is hard to see the interface between the bands, because the picture is not taken with confocal microscopy and the interface is curved. However the top part of the picture clearly shows a gelatin continuous phase (i.e. black spheres surrounded by white), while the bottom part clearly shows a dextran continuous phase (i.e. white spheres surrounded by black). Thus, the interface between the macroscopic bands in Figure 11a is indeed pictured in Figure 11b. More microscopic observations have shown that dark and light macroscopic bands like those in Figure 11a are respectively gelatin and dextran continuous at the outer wall of the set-up.

The problem is though that one cannot distinguish a state like the one shown in Figure 11a and a continuous phase inversion when using the cone-plate set-up, because it does not allow for macroscopic obervations. It has been mentioned before that banding seems to start at different shear rates for the two different shear set-ups. However, macroscopic observations have been made with the coaxial cylinder set-up that showed banding like in Figure 10 in only some regions of the set-up. It could be that the rheology in the cone-plate set-up is truly different from the one in the coaxial cylinder set-up, but verifying that hypothesis would need much more combined macroscopic and microscopic observations preferably in both shear set-ups. Also, until the rheology of the emulsions in the different shear set-ups are matched or are proved different, it is hard to defend Figure 8 as the final awnser to the behavior of the system under shear.

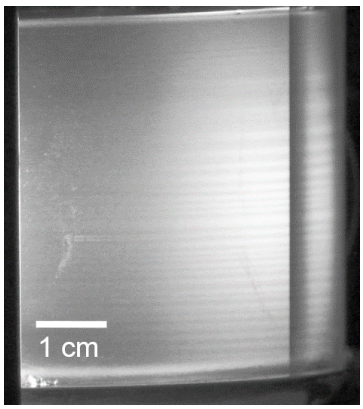

Figure 10: Picture of macroscopic bands in the coaxial cylinder set-up (dextran 2000 kDa : gelatin = 1 : 2, shear $20\,s^{-1}$).

5.1 Velocity profiles

Both confocal and normal fluorescence microscopy allow the sample to be studied to a depth of about $250\,\mu$m, while the sample depth in the gradient direction is up to 2 mm. Heterodyne light scattering is a good technique to overcome this restriction and a first step to verify whether the same things happen at the inner side of the gap and the outer side of the gap. A downside of this technique is that only single space- and time-averaged data points are gathered, unlike pictures that can show many small variations in flow and microscopic structure.

Figure 11c and 11d have been constructed from data gathered by heterodyne light scattering. In Figure 11c it can clearly be seen that the upper (darker) band scatters much more light than the lower (lighter) band. This correlates well with the microscopic observation seen in Figure 11b in the following way. The upper band has a gelatin rich phase continuous. The gelatin rich phase is more viscous than the dextran rich phase, so the upper (darker) band experiences a higher shear stress. A higher shear stress means smaller dispersed droplets, which gives rise to more turbidity and hence a darker appearance macroscopically.

The turbidity in either phase is mostly caused by scattering from the emulsion structure. Going along the line of the previous paragraph, regions in the sample that are higher in turbidity and scatter more strongly have a gelatin rich phase as the continuous phase. Figure 11c shows a lower scattering region in the middle of the sample, followed by a higher scattering region at the inner cylinder. This would suggest that a dextran continuous gradient band is present in the middle of the sample and a gelatin continuous gradient band at the inner cylinder of the sample, resembling something like Figure 7h. The velocity profile (Figure 11d) also shows an abrupt change slightly beyond the middle of the

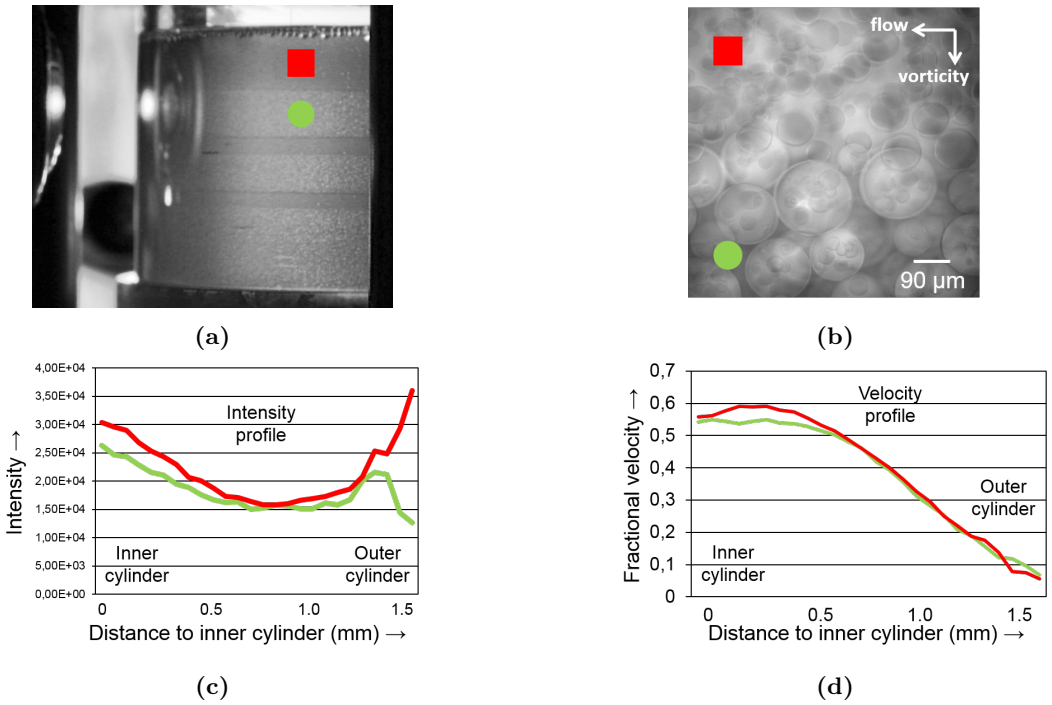

Figure 11: Pictures and data gathered from dextran 150 kDa : gelatin = 1 : 2 emulsions with shear: $1\,s^{-1}$. **(a)** Macroscopic image of the emulsion. **(b)** Microscopic picture of the emulsion taken where the microscope shines it's light on in (a). **(c)** Heterodyne light scattering intensity through the cylinder. **(d)** Fluid velocity devided by the theoretical velocity of a Newtonian fluid through the cylinder. **(c/d)** The upper, red profiles were taken through a band like the one marked with a red square in (a/b) and the lower green profiles were taken through a band like the one marked with a green circle in (a/b).

sample. This could well correlate with a change in continuous phase.

Also clearly visible in Figure 11d is that the velocity does not reach the theoretical value of 1. The inner cylinder is rotating, but the fluid region right next to it does not have the same velocity. This would mean wall slip is present at the inner cylinder, a known effect to viscous solutions [23]. Still, the wall slip explanation is uncertain as it has not been observed with gelatin/pullulan emulsions. It could be that pullulan containing samples are less prone to wall slip than dextran containing ones, but more research is necessary to verify this hypothesis.

Finally, it can be seen in Figure 11d that the gradient in velocity is lower and less constant at the outer cylinder, particularly in the profile which corresponds to the gelatin continuous region at the outer cylinder. A gelatin continuous wetting layer is usually present at the interface of glass and water in these emulsions as observed by confocal microscopy. The fluctuations in velocity at the outer cylinder could correspond to this wetting layer. Another observation is that this gradient becomes more like the rest of the velocity gradient measured in the sample when the shear rate is increased. This could correspond to the disappearing of the wetting layer at higher shear rates also reported in [20].

6 Inhomogeneity effects

In samples that form stable emulsion-like structures under shear (viscosity ratio smaller than unity; left hand side of Figure 8) it can be seen by confocal microscopy that all droplets on the same depth in the sample have the same velocity. The shear rate is then homogeneously distributed throughout the sample. In samples displaying wormlike banding, velocities of droplets at a single sample depth can differ a lot. This has also been reported in previous research concerning phase separated polymer solutions [7]. This would mean that the shear rate is not homogeneously distributed throughout the sample. This could correlate with the basic phase separation in bands with a different shear rate described in Ref. [24].

Another characteristic that can be seen in banding samples is that droplets inside dextran rich wormlike bands are clearly bigger and less deformed than droplets next to the wormlike band in the vorticity direction, Figure 12a. Also droplets above and below a dextran rich wormlike band in the gradient direction are bigger and less deformed than neighboring droplets in the vorticity direction, see Figure 12b. The droplet size can be correlated to the Laplace pressure and thereby the shear stress experienced by a droplet [14]. Therefore, these observations suggest that the shear stress is always

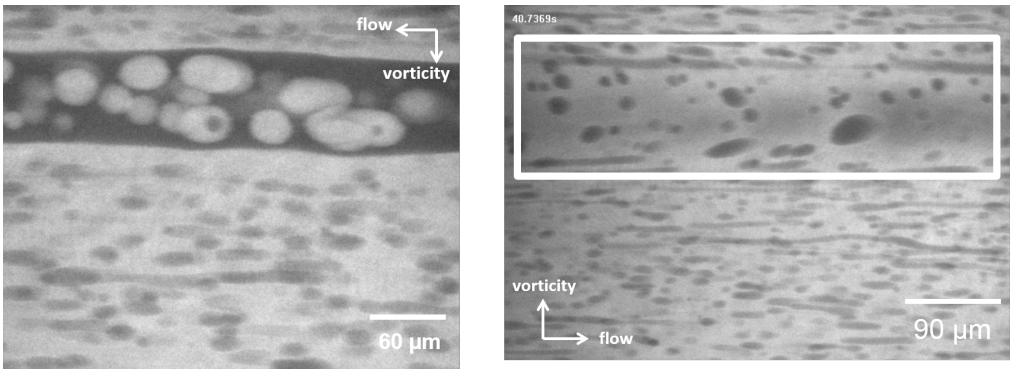

(a) **(b)**

Figure 12: **(a)** Droplets inside and outside a wormlike band differ in size (dextran 150 kDa : gelatin = 1 : 2, shear: $9\,s^{-1}$). **(b)** A rectangle has been set around the droplets just above a wormlike band in the gradient direction, these are also clearly different in size than those not above the band (dextran 150 kDa : gelatin = 1 : 3, shear $7.5\,s^{-1}$).

homogeneously distributed along the shear gradient direction in a sample and can be heterogeneously distributed in the vorticity direction. This has also been described for other shear banding samples [5].

The same seems to hold for gradient bands. Droplets inside and above or below a gradient band are the same size on average. When gradient bands break up into wormlike bands, the droplet size decreases in the gelatin rich continuous phase and increases in the dextran rich continuous phase.

6.1 Band flattening

The shape of the wormlike bands observed in this research is not perfectly torodial, which is preferential from a surface tension point of view. Instead, thick bands appear to be flattened in the gradient direction and stretched in the vorticity direction, Figure 13a and 13b. The cross section of wormlike bands are thus not circular, but tend to be elliptic when shear is present. The shape becomes less elliptic at lower shear rates or when stopping the shear completely, Figure 13c. Thus, wormlike bands strife to lower their surface area with the continuous phase, however at higher shear rates there appears to be a driving force to flatten them in the gradient direction, see Figure 14 for a schematic view.

As there is a competition between lowering the surface area at low shear rates and band flattening at higher shear rates, it seems likely that there is a competition between the Laplace pressure and the shear stress experienced by a banding sample. Both the Laplace pressure and the shear stress are pressures. Systems always try to lower their pressure, so a formula has been sought that minimizes the sum of these pressure for a given sample type. A complete derivation of this formula is given in the Appendix. A brief overview of the derivation is given below.

It will be assumed that only the Laplace pressure and the shear stress influence the bands, hydrodynamic constraints will be ignored as second-order effects. This assumption is likely to hold as long as the size of the bands does not approach the size of the shear gap. Secondly, it is assumed that every banded part of the sample behaves as a perfect gradient band. This means that the shear stress is equal at all points on a line in the shear gradient direction. Third, on the microscopic scale bands are shaped like infinitely long homogeneous rods in the flow direction, so the problem will be approximated as being 2-dimensional in the shear gradient/vorticity-plane. This makes the problem much easier to solve than for actual torus shaped bands.

In Equation 1 the average shear stress of a banded sample is given.

$$\bar{\tau} = \eta_\alpha \dot{\gamma} \left(1 + \frac{w}{W} \left(\frac{1}{\frac{2h}{\pi H}\left(\frac{\eta_\alpha}{\eta_\beta} - 1\right) + 1} - 1 \right) \right) \quad (1)$$

The part before the first bracket is simply the Newton equation for the shear stress, everything between the brackets is a correcting term for the banded part. The term w/W is the ratio between the band's width and the sample width, h/H is the ratio between the band's height and the sample height and η_α/η_β is the ratio between the viscosity of the continuous phase and the band's viscosity, the viscosity ratio.

The width w and height h of a band can be expressed as a function of each other, because the total surface area of a band β has to stay the same within the shear/vorticity-plane. By rewriting all bandwidths w to $(4\beta)/(\pi h)$, only h remains as a variable:

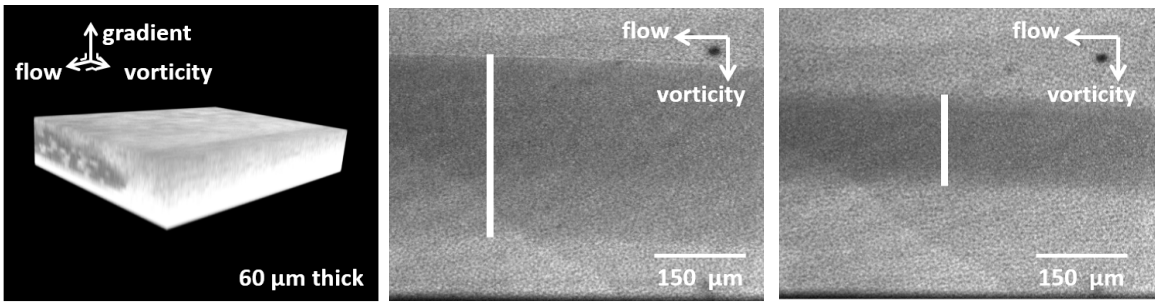

(a) **(b)** **(c)**

Figure 13: **(a)** Z-scan of a wormlike band flattened in the gradient direction and stretched in the vorticity direction (dextran 150 kDa : gelatin = 1 : 3, shear: $12\,s^{-1}$) **(b)** Picture of a flattened wormlike band (dextran 2000 kDa : gelatin = 1 : 2, shear: $18\,s^{-1}$) **(c)** Picture of the same band as in (b), but 30 seconds after cessation of the shear (dextran 2000 kDa : gelatin = 1 : 2, no shear)

$$\bar{\tau} = \eta_\alpha \dot{\gamma} \left(1 + \frac{4\beta}{\pi h W} \left(\frac{1}{\frac{2h}{\pi H}(\frac{\eta_\alpha}{\eta_\beta} - 1) + 1} - 1 \right) \right) \tag{2}$$

By differenting Equation 2 to h or by simply filling in some realistic numbers, it can be seen that the average shear stress indeed is reduced by flattening a band (i.e. decreasing h).

In Equation 3 the Laplace pressure of a band is given. (Note that γ is the surface tension between the band and the continuous phase and $\dot{\gamma}$ is the shear rate over the sample!)

$$\Delta P = \gamma \left(\frac{1}{w} + \frac{1}{h} \right) \tag{3}$$

In this rewritten Laplace formula w and h are not the radii of the band, but the respective diameters. This is because of the dimensional constraints of the problem. Again, see the appendix for a better elaborated argumentation.

An expression for the minimum pressure in a banded sample can be found by differentating the sum of the average shear stress and the Laplace pressure, Equation 4.

$$\frac{4\beta\eta_\alpha\dot{\gamma}h^2}{\pi W\gamma} = \left(1 - \frac{\pi h^2}{4\beta}\right)\left(h + \frac{\pi H}{2(\frac{\eta_\alpha}{\eta_\beta} - 1)}\right)^2 \tag{4}$$

This equation is of the form $0 = Ah^4 + Bh^3 + Ch^2 + Dh + E$ and can be solved analytically. The result of the analytcal solution is too big to put into this report, however. Still, the analytical solution and particular solutions can easily be obtained by the aid of computer programs.

In Figure 13a a 3-dimensional render of stacked confocal pictures (Z-scan) of half a band can be seen. By estimating the constants in Equation 4 for Figure 13a to $\beta = 12000\,\mu m^2$, $H = 2\,mm$, $W = 2\,mm$, $\dot{\gamma} = 12\,s^{-1}$, $\gamma = 0.1\,\mu N/m$ [7], $\eta_\alpha = 250\,mPa{\cdot}s$ and $\eta_\beta = 50\,mPa{\cdot}s$, then $w = 300\,\mu m$. This is close to the observed width of about $310\,\mu m$ (note that only half the band is visible in the picture). More measurements will have to be made to further verify equation 4.

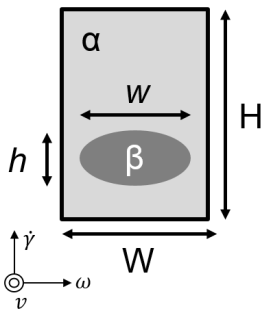

Figure 14: A schematic view in the flow direction of a wormlike band flattened by shear. α and β respectively denote the surface area of the continuous phase and the wormlike band in the shear gradient/vorticity plane, they are conserved quantities in the following derivation.

7 Discussion

In both Figure 9a and microscopy observations under shear (summarized in Figure 8) it can be seen that the system under shear prefers the less viscous phase to be continuous in spite of the less viscous phase not being the majority phase. Also, the continuous phase has a greater influence on the overall viscosity than the dispersed phase. These are known effects to literature and have been the subject of theoretical descriptions that predict overall viscosities of emulsions from viscosity ratio's [21, 22].

An emulsion tends to have the most abundant phase continuous at rest. However, under shearing conditions the phase which gives the lowest overall viscosity is continuous [18]. This corresponds to the

observations that emulsions can perform continuous phase inversion as a function of shear rate when the dispersed phase is less viscous than the continuous phase. These observations and knowledge from literature would suggest that having an even lower viscous dispersed phase should make continuous phase inversion more favorable. This would correspond to an increase of the dark grey zone in Figure 8. When going to a 1: 1 viscosity ratio the banding area (light grey) should disappear and zones of either continuity (dark grey and white) should be equal in size. There is an activation barrier present in the process of phase inversion as there is hysteresis in the shear rate of inversion.

All discussion presented above seems not to apply for the 2000 kDa dextran samples. There banding and deformation happens when gelatin is the most abundant and initially continuous phase, while it has a lower viscosity than dextran phase in this sample type. All other dextran weight samples (and pullulan) obey the rule that deformation, banding and/or inversion happens when the continuous phase is higher in viscosity than the dispersed phase. In an attempt to still hold up this rule of thumb it can be suggested that the viscosities of the dextran and gelatin phase change when they are mixed. Both phases contain water and the water concentration in a phase highly influences its viscosity (see the difference in absolute viscosities between Figure 9a and 9b). Osmosis-like processes driven by polymer swelling could invert the viscosity ratio in this sample, but this would have to be further verified with experiments.

How the diagram in Figure 8 would change with respect to varying the surface tension is not yet clear. The observed bands generally have a much lower surface-to-volume ratio than the surrounding droplets. In that sense, a higher surface tension should have the same effects as lowering the viscosity of the dispersed phase (banding at lower shear rates). Still, the formation of banding seems to require highly elongated droplets, a morphology in which the surface area is very high. Following this logic, a higher surface tension would inhibit banding and inversion. It could also be that both effects are present. This would make banding and inversion more favorable, but would also increase the activation barrier between the different states of the system. Which of the two influences is dominant and how this influences the behavior of the studied emulsions under shear, should be further investigated.

As a system under shear tends to minimize the shear stress it experiences in a shear rate controlled set-up [5], it seems plausible that the formation of wormlike or gradient bands make the sample less viscous, i.e. shear-thinning. This can also be deduced from the droplet sizes in- and outside of bands, Figure 12. Droplets inside or above a wormlike band in the shear gradient direction are bigger than those next to bands in the vorticity direction. This indicates that bands and the areas above and below them in the shear gradient direction experience a lower shear stress, because the average droplet size decreases with increasing shear stress through the Laplace pressure [14]. Experiencing a lower shear stress at the same shear rate means a lower viscosity, so banding indeed seems to shear-thin a sample.

Preliminary observations (Figure 13) and calculations (Equation 2) on the band flattening phenomenon indicate that flattened bands ($radius_{gradient} < radius_{vorticity}$) are lowering the shear stress further than isotropic bands.

Finally, the discrepancy between the results gathered from the cone-plate and the coaxial shear set-up need much more experiments to allow for a final discussion on the subject of structure formation in phase separated polymer solutions. Banding and inversion seem to happen at very different shear rates at the respective set-ups and macroscopic inhomogeneous effects have been observed in the coaxial shear set-up that can easily go unnoticed with the cone-plate set-up. But the the cone-plate data correlates too well with the gathered viscosity data to disregard any of the two data sets. More research will have to be performed to find the correct shear rates for structure formation or should verify that the two shear set-ups indeed produce different structures at the same shear rates.

8 Conclusions

The effects of shear on broken up (i.e. emulsified without emulsifier) phase separated polymer solutions have been studied in this research. Dispersed phases which are higher in viscosity than the continuous phase tend to form spherical droplets that become smaller with increasing shear rate. Low viscosity droplets also become smaller with increasing shear rates, but they become elongated in the process as well. Increasing the shear rate further will make these elongated droplets coalesce into wormlike shear bands. These bands span around the whole shear set-up in the flow direction, somewhat like a torus or donut. Wormlike bands have a lower surface/volume ratio than surrounding droplets, are stable under shear and gradually grow bigger when increasing the shear rate. Lowering or stopping the shear altogether makes them break-up into droplets through Rayleigh instabilities. Banding behavior starts at lower shear rates with samples that have a higher viscosity ratio.

The dispersed phase can become the continuous phase and vice versa in samples that have a dispersed phase that is lower in viscosity than the con-

tinuous phase. This typically happens at a shear rates higher than shear rates at which banding is observed. The continuous phase has a bigger influence on the overall viscosity of a sample than the dispersed phase. The change in viscosity with changing phase mass ratio's does not follow a lineair trend from one pure phase to the other (Figure 9a). Samples that have a lower viscous continuous phase have a lower overall viscosity than a lineair trend. Also, the change in viscosity per change in polymer fraction shows a steeper slope when there is a change in continuous phase.

With macroscopic observations and heterodyne light scattering it was observed that millimeter size banded structures can form in phase separated polymer solutions under shear. This makes it necessary to simultaneously observe both the macroscopic and microscopic structure of banding samples in future research if definite quantitative results are to be found for when samples start to form structures under shear.

Through droplet speed observations it could be deduced that the shear rate is inhomogeneous throughout a banded part of the sample. Average droplet sizes are clearly bigger in and just above (or below) bands in the shear gradient direction than at other parts in the sample. This means the Laplace pressure and thus the shear stress in and around bands is lower. Banding seems to be a way to lower the average shear stress experienced by the sample, this has also been theoretisezed in research on other banding samples [5]. Shear rates and shear stresses are thus not homogeneously distributed throughout a sample in a banding state.

The shape of the bands also seems to be able to influence the shear stress within a sample. An expression has been sought based upon Laplace pressure and shear stress within bands that predicted that flattened bands ($radius_{flow} < radius_{vorticity}$) are more favourable than isotropic bands. Gradient banding thus seems to able to lower the overall viscosity of a sample further than wormlike or vorticity bands.

9 Future work

The most straightforward objective for the future is obtaining graphs such as Figures 8 & 9a for more viscosity ratios. This should be done to further verify the more general properties of emulsions that have been concluded from this data. The research should include both macroscopic and microscopic observations, as macroscopic structures have been observed that cannot be distinguished by microscopy alone. Also, more long-term experiments should be conducted to investigate a possible memory function of the sample with respect to band formation and to verify whether there really is a hysteresis in band formation or bigger bands just take longer to break down.

The distribution of shear rates and strains in samples has until now mostly been observed indirectly. More heterodyne experiment should be conducted to verify how shear rates and strains are quantitatively distributed through the sample. In this research data was found for some sample types that could suggest wall slip, so an awnser should be sought whether this data is really produced by wall slip and why other samples do not perform this kind of behavior.

The effect of band flattening seems reproducible and further investigation could give insight into the formation of gradient bands by flattening of wormlike bands. The expression derived in this research gives a qualitative good prediction of band flattening and it should be tested whether the expression holds quantitatively and to what limits it can be pushed macroscopically.

The samples containing 2000 kDa dextran display behavior in the opposite viscosity ratio than other sample types. It could be that the dextran phase takes water from the gelatin phase and so the viscosity ratio changes. This hypothesis should be checked. A way to check this could be qualitative or quantitative IR-measurements. The signal from a pure dextran solution should be compared to one that is in equilibrium with a same mass percentage gelatin solution. The dextran phase should dilute if it indeed takes water from the gelatin phase and thereby lowers its viscosity.

Diluting the 20 % polymer emulsions of 150 kDa dextran yielded 15 % polymer emulsions. In these samples the pure lower viscous solution was higher in viscosty than some of the emulsions that had a higher viscous dispersed phase in them 9b. This is counter-intuitive and goes against theories on the subject [21, 22]. It could be that at lower polymer fractions the polymers in the continuous phase start to swell and so take water from the dispersed phase by an osmosis-like process. It could also be that the interfaces between the two phases are depleted from polymers, creating a layer of pure water in between them which has a very low viscosity. Still, for all given hypotheses more research would have to be done to verify any. Any awnser should also be able to explain why this process is not observed at 20 % polymer emulsions.

Finally, but not trivially, an answer should be sought for the paradox of bands that grow but never seem to coalesce. A process like Ostwald ripening is possible, but needs much more experimentation to verify.

Acknowledgements

The author would like to thank the staff and students at NIZO Food Research, Utrecht University and Forschungszentrum Jülich for scientific and non-scientific help and discussions throughout the project. "*All animals are equal, but some animals are more equal than others*" (George Orwell, *Animal Farm*, 1945): dr. Pavlik Lettinga is thanked for daily supervision in Jülich, Saskia de Jong is thanked for help with the viscosity measurements and dr. Hartmut Kriegs is thanked for help with the heterodyne experiments and H. Jan Klok is thanked for help with the microscopy experiments.

References

[1] N.J. Wagner, J.F. Brady, *Phys. Today*, **62**, 27-32 (2009).

[2] P.D. Olmsted, *Rheol. Acta*, **47**, 283-300 (2008).

[3] I. Cohen, B. Davidovitch, A.B. Schofield, M.P. Brenner, D.A. Weitz *Phys. Rev. Lett.*, **97**, 215502 (2006).

[4] S.M. Fielding, *Soft Matter*, **3**, 1262-1279 (2007).

[5] J.K.G. Dhont, W.J. Briels, *Rheol. Acta*, **47**, 257-281 (2008).

[6] L. Hilliou, D. Vlassapoulos, *Ind. Eng. Chem. Res.*, **41**, 6246-6255 (2002).

[7] R.H. Tromp, E.H.A.,de Hoog, *Phys. Rev. E*, **77**, 031503 (2008).

[8] T. Hashimoto, K. Matsuzaka, E. Moses, A. Onuki, *Phys. Rev. Lett.*, **74**, 126-129 (1995).

[9] C.C. Han, Y. Yao, R. Zhang, E.K. Hobbie, *Polymer*, **47**, 3271-3286 (2006).

[10] D.N. Broseta, L. Leibler, L.O. Kaddour, C. Strazielle, *J. Chem. Phys.*, **87**, 7248-7256 (1987).

[11] P. Walstra, **Physical Chemistry of Foods**, *CRC Press* (2002).

[12] T.G. Mezger, **Handbook of Rheology**, *Vincentz Network GmbH & Co KG* (2006).

[13] H.S. Jeon, E.K. Hobbie, *Phys. Rev. E*, **63**, 061403 (2001).

[14] P. Walstra, *Chem. Eng. Sci.*, **48**, 333-349 (1993).

[15] J.M.H. Janssen, **Dynamics of Liquid-Liquid Mixing**, *Ph.D. Thesis*, Eindhoven University of Technology: The Netherlands (1993).

[16] A. Onuki, *J. Phys.: Condens. Matter*, **9**, 6119-6157 (1997).

[17] P.H.M. Elemans, **Modeling of the processing of incompatible polymers**, *Ph.D. Thesis*, Eindhoven University of Technology: The Netherlands (1989).

[18] L.A. Utracki, *J. Rheol.*, **35**, 1615 (1991).

[19] H.H. Winter, **Rheometry with capillary rheometers**, *Encyclopedia of Life Support Systems* (2008).

[20] C. Lundell, E.H.A. de Hoog, R.H. Tromp, A.-M. Hermansson, *J. Colloid Interface Sci.*, **288**, 222-229 (2005).

[21] I.M. Krieger, T.J. Dougherty, *Trans. Soc. Rheol. III*, 137-152 (1959).

[22] S.J. Choi, W.R. Schowalder, *Phys. Fluids*, **18**, 420-427 (1975).

[23] H.A. Barnes, *J. Non-Newtonian Fluid Mech.*, **56**, 221-251 (1995).

[24] J.-B. Salmon, A. Colin, S. Manneville, *Phys. Rev. Lett.*, **90**, 228303 (2003).

A Band Flattening

Below a derivation will be given of Equation 4, which describes the measure of wormlike band flattening in the gradient direction (and stretching in the vorticity direction). A schematic overview of the phenomenon is shown in Figure 14. Wormlike bands are shaped like thin donuts macroscopically, but they appear as long elongated bands at the scale the problem is looked at. To simplify the problem, the sample will be treated as a medium with one endlessly long band present in it. Also, it will be assumed that the fluid performs pure gradient banding behavior. This means that the shear stress is equal for all points in a sample that lie on the same line in the shear gradient direction. Hydrodynamic constraints and other second order flow effects will be ignored. Apart from the gradient banding behavior, the fluid will be assumed to behave Newtonian (i.e. no wall slip, no shear thinning etc.).

A.1 Average shear stress

The Newton equation for shear stress reads:

$$\tau = \eta\dot{\gamma}$$

Here τ is the shear stress, η the viscosity of the sheared fluid and $\dot{\gamma}$ the shear rate. As pure gradient banding was assumed, it can be said that for a banded part of the sample the following shear stress equations hold:

$$\tau_\alpha = \tau_\beta$$

$$\eta_\alpha\dot{\gamma}_\alpha = \eta_\beta\dot{\gamma}_\beta$$

The subscript indicate for which phase the variable applies.

Whatever the viscosities and shear rates in the respective phases may be, the weighed average of the shear rates have to add up to the overall shear rate:

$$\dot{\gamma} = \frac{H - h(x)}{H}\dot{\gamma}_\alpha + \frac{h(x)}{H}\dot{\gamma}_\beta$$

The constant H is the height of the sample and the variable $h(x)$ is the height of the band on a point x in the vorticity direction. Now $\dot{\gamma}_\beta$ can be expressed as:

$$\dot{\gamma}_\beta = \frac{H}{h(x)}\dot{\gamma} - \frac{H - h(x)}{h(x)}\dot{\gamma}_\alpha$$

This equation can be put into the shear stress equation shown above ($\eta_\alpha\dot{\gamma}_\alpha = \eta_\beta\dot{\gamma}_\beta$):

$$\eta_\alpha\dot{\gamma}_\alpha = \eta_\beta\left(\frac{H}{h(x)}\dot{\gamma} - \frac{H - h(x)}{h(x)}\dot{\gamma}_\alpha\right)$$

Rewriting yields:

$$\dot{\gamma}_\alpha = \frac{\dot{\gamma}\frac{H}{h(x)}\eta_\beta}{\eta_\alpha + \frac{H-h(x)}{h(x)}\eta_\beta}$$

Filling this back into shear stress equation ($\eta_\alpha\dot{\gamma}_\alpha = \eta_\beta\dot{\gamma}_\beta$) gives:

$$\tau(x) = \frac{\eta_\alpha\dot{\gamma}\frac{H}{h(x)}\eta_\beta}{\eta_\alpha + \frac{H-h(x)}{h(x)}\eta_\beta}$$

This can be rewritten to:

$$\tau(x) = \frac{\eta_\alpha\dot{\gamma}}{\frac{h(x)}{H}(\frac{\eta_\alpha}{\eta_\beta} - 1) + 1}$$

This is an equation for the shear stress with only one variable $h(x)$, but this variable is in itself a function. Geometry dictates that for any circle or ellipse:

$$h(x) = h\sqrt{1 - \frac{4x^2}{w^2}}$$

Here h is the diameter of the band in the shear gradient direction and w the diameter in the vorticity direction. The origin of the coordinate system is set in the center of the ellipse. Filling this equation into the previous equation yields:

$$\tau(x) = \frac{\eta_\alpha\dot{\gamma}}{\frac{h}{H}\sqrt{1 - \frac{4x^2}{w^2}}(\frac{\eta_\alpha}{\eta_\beta} - 1) + 1}$$

This is a solvable equation for the shear stress for any point on the vorticity direction in a banded sample. To obtain the average shear stress in the sample, the equation has to be integrated over the sample width W and then divided by the width:

$$\bar{\tau} = \frac{\int_{-W/2}^{W/2}\tau(x)dx}{W}$$

Wolfram|Alpha was used to solve this equation and rewriting yielded:

$$\bar{\tau} = \eta_\alpha\dot{\gamma}\left(\frac{W - w}{W} + \frac{\pi w}{\frac{2h}{H}(\frac{\eta_\alpha}{\eta_\beta} - 1)W}\right) + C$$

Where C is the integration constant. By applying simple logic, it follows that $\bar{\tau} = \eta_\alpha\dot{\gamma}$ when either $h = 0$, $w = 0$ or $\eta_\alpha = \eta_\beta$. Imposing these limits on the above equation yields:

$$\bar{\tau} = \eta_\alpha\dot{\gamma}\left(\frac{W - w}{W} + \frac{\pi w}{(\frac{2h}{H}(\frac{\eta_\alpha}{\eta_\beta} - 1) + \pi)W}\right)$$

Rewriting this equation yields the equation for the average shear stress of a banded sample, Equation 1:

$$\bar{\tau} = \eta_\alpha \dot{\gamma} \left(1 + \frac{w}{W} \left(\frac{1}{\frac{2h}{\pi H}(\frac{\eta_\alpha}{\eta_\beta} - 1) + 1} - 1 \right) \right)$$

A.2 Laplace pressure

The Laplace pressure for droplets reads:

$$\Delta P = \gamma \left(\frac{1}{R_1} + \frac{1}{R_2} \right)$$

In which γ is the surface tension and R_1 & R_2 the radii of the droplet. Bands can be considered as endlessly deformed droplets. Then R_2 becomes ∞ and makes the second term between the brackets negligibly small and leaves the equation as a 2-dimensional Laplace pressure:

$$\Delta P = \frac{\gamma}{R}$$

Still the other two radii should be able to vary from each other as the final equation should be capable of describing flattend bands as well as perfectly torodial bands. The Laplace pressure is defined as the derivative of the surface area devided by the derivative of the volume. This would degenerate to the derivative of the circumfence devided by the derivative of the surface area in this 2-dimensional case. There is no analytical expression for the circumfence of an ellipse. The exact infinte series has been approximated by taking the average of the two radii and adding correcting factors. In this derivation we will use only the average of the two radii and neglect the correcting terms, as we focus on first order effects. The Laplace pressure for deformed ellipses (i.e. flattened bands) then becomes:

$$\Delta P = \frac{\gamma}{2} \left(\frac{1}{R_1} + \frac{1}{R_3} \right)$$

Recognizing that the radii are half the band's width $w/2$ and half the band's heigth $h/2$, the Laplace pressure for flattened bands reads as Equation 3:

$$\Delta P = \gamma \left(\frac{1}{w} + \frac{1}{h} \right)$$

A.3 Stress minimalization

Both the shear stess and Laplace pressure exert stress on the system. Before the minimization of this stress it is first necessary that only one variable is present in the equations, now both the width w and heigth h can vary when a band is flattened. The surface area of the cross section of a band β is a constant though and connects the width to the height via the equation for the surface area of an ellipse:

$$\beta = \frac{\pi}{4} wh$$

Now either all widths or heights of a band can be rewritten in terms of one another and some constants. Here the width has been chosen to be rewritten, making the equations of the average shear stress and Laplace pressure respectivaly:

$$\bar{\tau} = \eta_\alpha \dot{\gamma} \left(1 + \frac{4\beta}{\pi h W} \left(\frac{1}{\frac{2h}{\pi H}(\frac{\eta_\alpha}{\eta_\beta} - 1) + 1} - 1 \right) \right)$$

$$\Delta P = \gamma \left(\frac{\pi h}{4\beta} + \frac{1}{h} \right)$$

The band height h for minimum first order stress in a banded sample can now be found by taking the derivative of the sum of the two equations above to h and then finding at which value of h the resulting equation is zero:

$$\frac{\delta(\bar{\tau} + \Delta P)}{\delta h} = 0$$

Solving this equation does not require more than algebra. This has not been fully written out, because the process does give any more insight, but would take up a lot of space. The end result reads as Equation 4:

$$\frac{4\beta\eta_\alpha\dot{\gamma}h^2}{\pi W\gamma} = \left(1 - \frac{\pi h^2}{4\beta}\right) \left(h + \frac{\pi H}{2(\frac{\eta_\alpha}{\eta_\beta} - 1)} \right)^2$$

This equation only has h as a variable and can be rewritten to the form $0 = Ah^4 + Bh^3 + Ch^2 + Dh + E$. Fourth-power equations can be solved analytically, but again the process and end result give no further insight into the phenomenon of band flattening. The result can however be put into computer programs to predict the height of a flattened band (and also the width of a band by rewriting).